ARTICLE

OBC
www.rsc.org/obc

The mechanism and regioselectivity of the ene reactions of nitroso compounds: a theoretical study of reactivity, regioselectivity, and kinetic isotope effects establishes a stepwise path involving polarized diradical intermediates

Andrew G. Leach and K. N. Houk *
Department of Chemistry and Biochemistry, University of California, Los Angeles, California 90095-1569, USA. E-mail: houk@chem.ucla.edu

Received 10th January 2003, Accepted 6th March 2003
First published as an Advance Article on the web 26th March 2003

A theoretical study of the mechanisms of ene reactions of nitroso compounds has been completed, using UB3LYP, CASPT2, UCCSD(T) and UQCISD(T) methods. Stepwise paths through polarized diradical intermediates are always preferred. These intermediates have unusual properties, involving high rotational barriers about formally single bonds, which permit them to maintain stereochemical relationships. The diradicals may exchange the RNO moiety between the two ends of the alkene *via* an aziridine *N*-oxide. The aziridine *N*-oxide cannot be accessed directly from reactants and cannot lead directly to ene products. It is therefore an innocent by-stander in the way proposed by Singleton for the aziridinium imide in the ene reactions of triazolinediones. A detailed analysis of the electronic structure of the polarized diradicals is given. The kinetic isotope effects measured in a Stephenson isotope effect test have been reproduced. These kinetic isotope effects are consistent with a mechanism in which partitioning of the polarized diradical between cyclization to an aziridine *N*-oxide and H-abstraction to ene product takes place, and in which the formation of the polarized diradical is to some extent reversible. Finally, calculated regioselectivities reproduce those observed experimentally.

Introduction

The drive to understand the details of the mechanism of the ene reactions of highly electrophilic heteroenophiles, such as singlet oxygen, nitroso compounds and triazolinediones has provided the impetus for both experimental and theoretical studies of these reactions.[1] The ene reaction of singlet oxygen has been of interest to this group for several decades.[2] These three types of enophiles have many mechanistic possibilities open to them, the concerted, Woodward–Hoffmann allowed reaction, or else their highly electrophilic nature may divert them to stepwise mechanisms instead. All three share a combined electrophile–nucleophile potential. The electrophilicity is due to a low-lying π* orbital and nucleophilicity to an orthogonal high-lying filled π* or lone-pair type orbital.[1]

An extension of our theoretical studies to the ene reactions of nitroso compounds has been made. These reactions preferentially proceed through polarized diradical intermediates. This intermediate may either abstract a hydrogen directly to yield the ene product or may cyclize to form an aziridine *N*-oxide. In the latter case, it may only achieve an ene reaction by subsequently reopening to reform a polarized diradical. The polarized diradical does not readily undergo rotation about formally single bonds due to a weak C–N bonding interaction and to CH–O hydrogen bonding. These mechanistic details have been confirmed with a range of theoretical methods which lead to a detailed description of the electronic structure of the intermediate. The proposed mechanism provides startlingly good agreement with experimental kinetic isotope effects and regioselectivity.

Background

Until recently, the ene reactions of nitroso compounds received little attention, either experimental or theoretical.[3] Recently, milder ways of generating these compounds have been developed;[4] these have led to an increased interest in their reactions both as dienophiles in the hetero-Diels–Alder reaction[5] and as enophiles in the ene reaction.[5d,6] The ene reactions of nitroso compounds of electron poor aromatic species, such as chloro or acyl nitroso compounds are rapid, yield reasonably stable products, and are highly regioselective.[7,8] The hydrogen that is abstracted in the ene reaction of trisubstituted alkenes is generally one of those named *twix* by Adam, from the substituent on both the most crowded end of the double bond and the most crowded side (Scheme 1).[8] This is in contrast to the ene reactions of singlet oxygen which abstract from the most crowded side of the double bond with little selectivity between the two ends of the alkene.[8] The ene reactions of triazolinediones are selective for hydrogen abstraction at the most crowded end of the alkene with little selectivity between the two sides.[8] These two latter classes of enophile have been the subject of many experimental and theoretical studies.[9]

Nitroso compounds, like singlet oxygen and triazolinediones, are highly electrophilic. HNO has a computational Parr electrophilicity index of 3.01 eV while acrolein, the acrolein–BH_3 complex, singlet oxygen and triazolinedione have Parr electrophilicty indices of 1.84 eV, 3.20 eV, 3.77 eV and 4.77 eV respectively.[10] Like singlet oxygen and triazolinediones, nitroso compounds can also be effective nucleophiles – their HOMOs are high energy antibonding combinations of N and O lone pairs, orthogonal to the low energy π* LUMO which is responsible for their electrophilicity (Fig. 1).

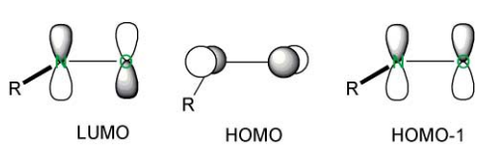

Fig. 1 Frontier molecular orbitals of nitroso compounds.

There are a range of plausible mechanisms for these, and most, ene reactions (Scheme 2). This includes the concerted one and stepwise paths involving either diradical, zwitterionic, 3-membered-ring aziridine *N*-oxides or 4-membered ring

DOI: 10.1039/b300285c

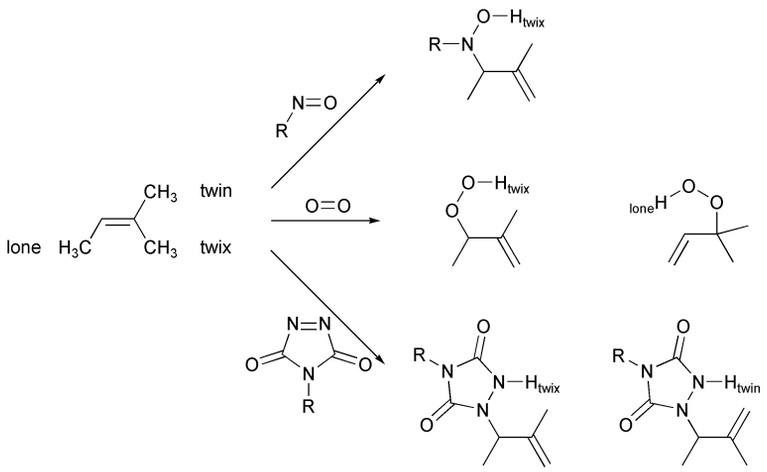

Scheme 1 The regioselectivity of the electrophilic enophiles nitroso compounds, singlet oxygen and triazoline diones. The nomenclature for regioselectivity is that adopted by Adam *et al*.[8]

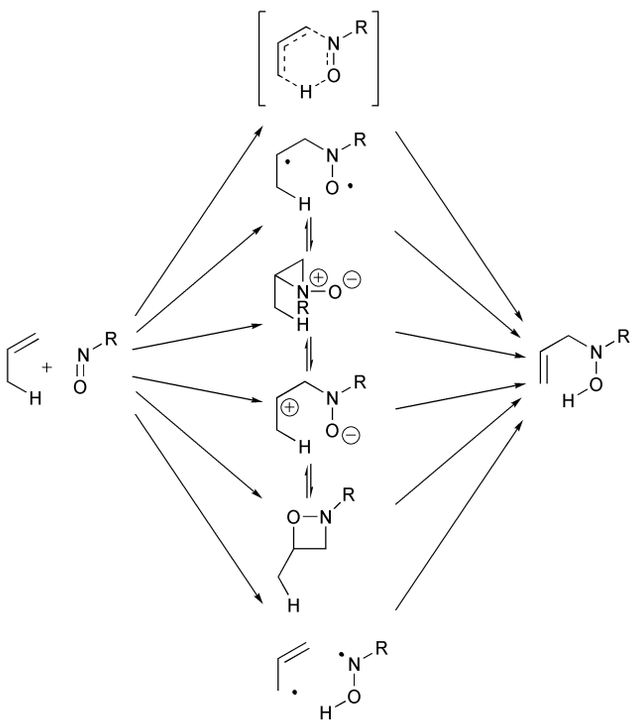

Scheme 2 Possible mechanisms for the ene reaction of nitroso compounds.

oxazetidine intermediates. Further complication arises from the possibility that diradicals or zwitterions could close to form aziridine *N*-oxides. An alternative stepwise mechanism in which the first step is a hydrogen abstraction by the oxygen of the nitroso compound to generate two radicals which then combine is also possible. In principle, reactions in which the allylic proton is abstracted by nitrogen with formation of a C–O bond are also possible, but the products of such reactions have not been observed and PM3 calculations were unable to locate any structures corresponding to this possibility.[11]

Some mechanistic studies have been reported. Seymour and Greene measured the intra- and inter-molecular kinetic isotope effects for the reaction between pentafluoronitrosobenzene and tetramethylethylene (TME).[12] They deduced that the reaction must involve a species with the symmetry of an aziridine *N*-oxide and speculated that the most likely candidate is the aziridine *N*-oxide itself. Recently, Adam *et al.* have remeasured these isotope effects and proposed a substantially revised value for the intermolecular isotope effect.[13] They argued that the kinetic isotope effects are consistent with reversible formation of an aziridine *N*-oxide.

Davies and Schiesser performed PM3 level calculations on the reaction of HNO with propene and also concluded that the path leading from reactants to aziridine *N*-oxide and thence to products is lower than its concerted counterpart.[11] They proposed a rationale for the regioselectivities based on the HOMO diene–LUMO HNO interaction (Fig. 2). They envisaged that the preference for electrophiles such as HNO to react at the most nucleophilic (least substituted) end of an alkene could also influence the stability of the two regioisomeric transition states linking an aziridine *N*-oxide to ene reaction products. Although this could explain the selectivity for abstraction from the most crowded end of the alkene, it does not address the selectivity between the two sides.

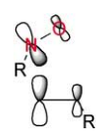

Fig. 2 Proposed frontier molecular orbital rationalization for the regioselectivity of the ene reaction of nitroso compounds.[11]

Adam has proposed a model for regioselectivity based on a "skew" preference in the relevant transition state.[8] Here, the nitroso compound approaches such that the substituent on nitrogen lies in the emptiest region of space around the alkene, near the less substituted terminus of a trisubstituted alkene. The remainder of the nitroso compound then prefers to lie diagonally across the rest of the alkene and is steered towards twix abstraction (Fig. 3). This was validated by a series of B3LYP/6-31+G* calculations which predicted that such transition states would exist as part of a stepwise mechanism involving the intermediacy of an aziridine *N*-oxide.[14] A revisitation of their calculations has found them to be incomplete. The skew transition state model is too simplistic.

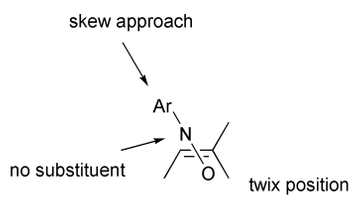

Fig. 3 Adam's "skew transition state" explanation for regioselectivity for the ene reactions of nitroso compounds.[8]

As part of an ongoing interest in the reactions of nitroso compounds, theoretical investigations of the Diels–Alder reactions of these compounds[15,16] and the thermochemistry of HNO and its relevance to biochemistry have been reported previously.[17] Diels–Alder reactions involving nitroso compounds

as dienophiles follow a concerted path involving highly asynchronous transition states.[15] Of the two stereoisomeric concerted transition states, the *endo* is preferred as it minimizes the repulsive interactions between the N and O lone pairs and the electron rich diene. A stepwise path through diradical intermediates was found to be several kcal mol^{-1} above the lowest energy concerted path in all cases. This difference in energy was larger if the nitroso compound included a larger substituent on nitrogen and in the absence of radical stabilizing substituents on the diene. Computational investigations of HNO have led to a revised pK_a and showed that HNO would exist in physiological conditions as the protonated, unhydrated form.[17]

Computational methods

B3LYP/6-31G* calculations were performed with Gaussian 98.[18] These employed the hybrid exchange functional of Becke[19] and the correlation functional of Lee, Yang and Parr.[20] Unrestricted calculations began with an initial guess in which HOMO and LUMO were mixed to break spatial symmetry of the orbitals. The resulting calculations involve a spin contaminated wavefunction in which $<S^2> \neq 0$, due to admixture of high spin states into the singlet. This can be eliminated using the spin projection method of Yamaguchi *et al.*[21] Some have questioned the meaning of the value of $<S^2>$ in UDFT and advocated using uncorrected energies.[22] Spin projection is certainly beneficial in some cases.[23]

Potential energy surfaces were obtained using the redundant coordinates feature in Gaussian 98 to calculate the optimized geometry and energy for a structure in which two interatomic distances were constrained. NBO charges were calculated in Gaussian 98.[24]

CCSD(T) and QCISD(T) calculations were also performed in Gaussian 98.[18] Spin projection in these calculations was performed using the natural orbital analysis method advocated by Isobe *et al.* for estimating the value of $<S^2>$ for a QCISD single point and assuming that this is the same value as for QCISD(T) and CCSD(T).[25] A subsequent triplet single point calculation provides the remaining information necessary for spin projection using the Yamaguchi *et al.* method.[21]

CASPT2 calculations were performed with MOLCAS 5.[26] The CASPT2 calculations apply a second order perturbation theory correction to a CASSCF calculation. The CASSCF calculation involved a 10 electron, 8 orbital active space. These orbitals were the C–N σ and σ*, NO σ and σ*, NO π and π* and, O 2p and O 2s orbitals (the electrons corresponding to the two lone pairs of the reactant nitroso compound) in the diradical, and the corresponding orbitals in each of the other species. The exception was the product, in which the 8 orbitals included the C–C π and π* orbitals, NO σ and σ*, CN σ and σ*, the lone pair on N and only one of the O lone pairs (in a p type orbital). CASSCF optimization was performed with Gaussian 98 using the same active space. Solvation calculations utilized the PCM method of Tomasi *et al.*[27] and were performed in Gaussian 98.[18]

Kinetic isotope effects were calculated using B3LYP/6-31G* frequencies scaled by 0.9613.[28] These calculations employed the program QUIVER[29] and had the temperature set to 263 K, corresponding to the experimental temperature.[12] For steps not involving hydrogen transfer, the Bell tunnelling correction was applied.[30]

Results and discussion

Mechanism

In order to gain a foothold in the complex mechanistic terrain already outlined, the aziridine *N*-oxide that is formed in the reaction between HNO and propene was chosen as a starting point for calculations to generate two potential energy surfaces. The aziridine *N*-oxide was optimized with RB3LYP/6-31G*. The potential energy surfaces were calculated using a series of constrained optimizations and the RB3LYP/6-31G* method. Important turning points were subsequently optimized with UB3LYP to establish their stability with respect to the closed shell restriction of RB3LYP.

The first potential energy surface was defined by the lengths of the two C–N bonds of the aziridine *N*-oxide ring. The possible pathways linking the aziridine *N*-oxide to reactant (alkene and nitroso compound, HNO) are described by this surface. This potential energy surface shown in Fig. 4 established that with B3LYP/6-31G* a concerted path linking reactants to aziridine *N*-oxide is much more difficult than a stepwise path. The concerted path runs along the diagonal of the surface shown in Fig. 4. The formation of an aziridine *N*-oxide proceeds instead through an open chain intermediate, formed by C–N bond formation at the least substituted end of the alkene, presumably reflecting the greater stability of a secondary radical or cation compared to a primary one.

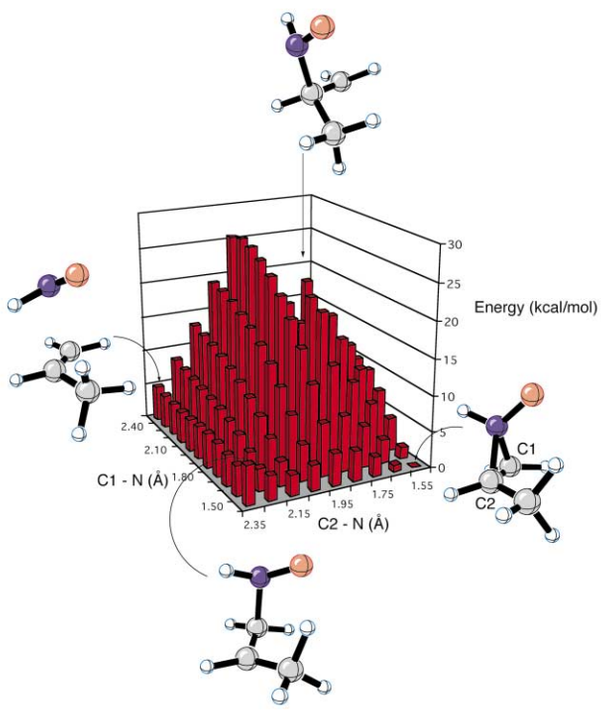

Fig. 4 RB3LYP/6-31G* potential energy surface linking aziridine *N*-oxide to reactant nitroso compound (HNO) and propene.

The second potential energy surface, shown in Fig. 5, also calculated using RB3LYP links the aziridine *N*-oxide to the hydroxylamine product. It is defined by the C2–N distance and the O–H (where H is the hydrogen to be abstracted) distance. The diagonal corresponding to a concerted transition state for the formation of products from the aziridine *N*-oxide is again relatively high in energy. Product formation proceeds through ring opening to an open chain intermediate and subsequent hydrogen abstraction. The C–N bond to the most substituted carbon atom breaks preferentially, again reflecting the greater stability of a secondary radical or cation compared to primary.

A transition state for the one step, concerted ene reaction could not be located. A potential energy surface mapping the conversion of reactants directly to ene products showed that no such transition state is present on the RB3LYP surface. The mechanism in which the nitroso oxygen first abstracts an allylic hydrogen to generate an allyl radical and a hydroxyaminyl radical was shown unlikely because the two radicals were calculated to be at 25.8 kcal mol^{-1}. This is 22 kcal mol^{-1} higher than any of the transition states calculated for the mechanism involving a diradical intermediate.

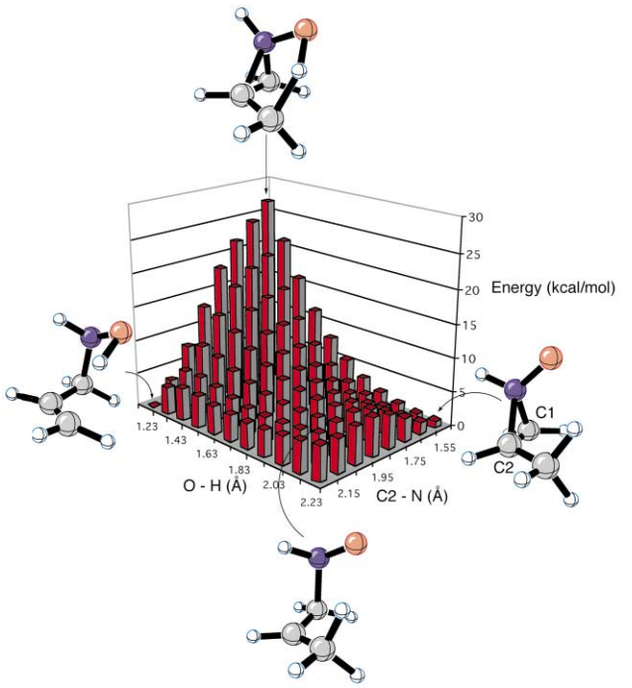

Fig. 5 RB3LYP/6-31G* potential energy surface linking aziridine *N*-oxide to ene product.

The potential energy surface scans demonstrated that the reaction of HNO with propene must proceed through an open chain intermediate that may cyclize to a 3-membered ring aziridine *N*-oxide or proceed to the ene product. Each of the stationary points that was identified by these scans was optimized with RB3LYP/6-31G* and UB3LYP/6-31G*. This established that the open chain intermediate has a great deal of diradical character. However, these species could also be optimized with spin restricted calculations suggesting some highly polar character, the nature of this species will be discussed below. The B3LYP/6-31G* diradical has $<S^2>$ = 0.6, while all other species, including the transition states linking the diradical to reactant, products or aziridine *N*-oxide have $<S^2>$ = 0. Restricted and unrestricted calculations yield identical structures for all species except for the diradical itself. Without the aid of potential energy surface scans, it would have been easy to overlook this intermediate. The B3LYP/6-31G* energetics of this reaction, and the geometries of the key species are presented in Scheme 3.

Spin projection lowers the diradical energy to a value of 1.9 kcal mol^{-1} below that of reactants. While this is a satisfactory picture of the mechanism, a recent study showed that B3LYP can provide an incorrect description of the reaction mechanism for some reactions involving heteroatomic radicals.[31] This led us to perform a series of single point calculations at a range of theoretical levels to determine if the mechanism and energetics found with B3LYP are valid.

Energies of each of the UB3LYP/6-31G* geometries with a number of methods were established. These methods were UQCISD(T)/6-31G**, UCCSD(T)/6-31G**, UCCSD(T)/6-311+G** and CASPT2/6-31G**. The CASPT2 calculations were based on CASSCF(10,8) calculations.

The enthalpies of each species shown in Scheme 3, calculated using B3LYP/6-31G* corrections to the electronic energy, are shown in Table 1. While the methods diverge as to the absolute magnitude of the barriers, they agree upon the relative positioning of the three key transition states and the diradical. All methods predict that the intermediate is lower in energy than the transition states leading to it and therefore all agree upon its existence as a minimum. The data in Table 1 show B3LYP/6-31G* and CASPT2/6-31G** are in reasonable agreement with each other. The other methods position all species approximately 10 kcal mol^{-1} higher in energy above the reactants. Methods such as QCISD(T) and CCSD(T) with very large basis sets are often employed as benchmarks for other "lower level" calculations, but their reliability for open shell systems remains largely untested.[32] Isobe *et al.* have recently suggested that spin contamination remains a problem for these methods and proposed a scheme of spin projection based on natural orbital populations for UQCISD single point calculations.[25] $<S^2>$ is calculated for the contaminated singlet by using natural orbital populations. A triplet single point is then performed and the usual Yamaguchi spin projection protocol applied.[21] The same energy projections are employed for UQCISD(T) and UCCSD(T) calculations. While this procedure is somewhat unsatisfactory, it provides an estimate of the errors caused by spin contamination in these calculations. The corrected values calculated in this way are also shown in Table 1. It can be seen that these are, by and large, in excellent agreement with those calculated by B3LYP and CASPT2 for the transition states and

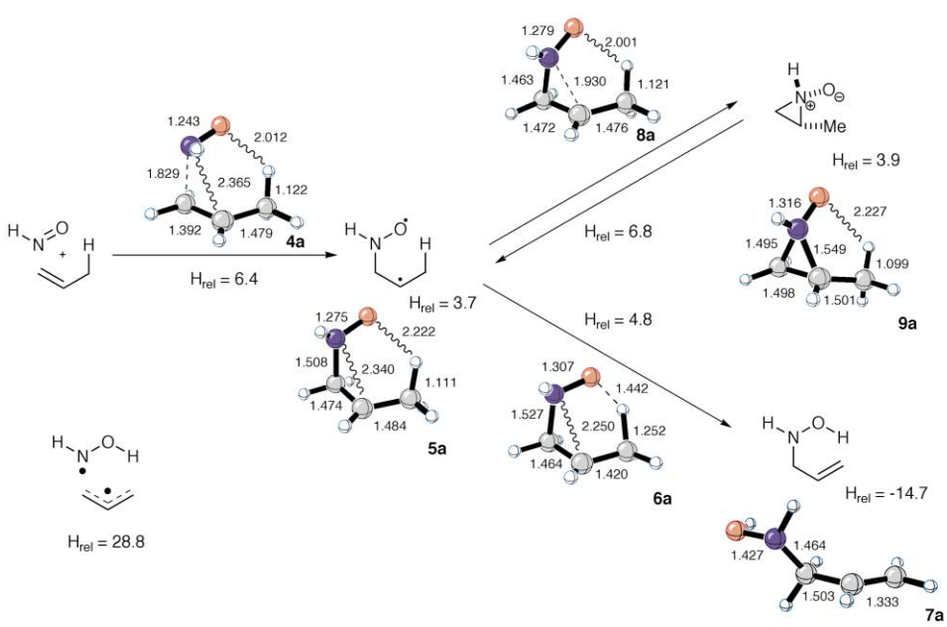

Scheme 3 The B3LYP/6-31G* mechanism for the ene reaction between HNO and propene.

Table 1 Energetics for the ene reaction between HNO and propene computed by B3LYP/6-31G* and a series of single point energy evaluations on the B3LYP/6-31G* structures. Spin projected energies are in parentheses. Energies are reported in kcal mol^{-1}

Method	**4a**	**5a**	**6a**	**7a**	**8a**	**9a**
B3LYP/6-31G*	6.4	3.7 (−1.9)	4.8	−14.7	6.8	3.9
UQCISD(T)/6-31G**	16.6 (8.7)	12.9 (4.5)	14.5 (5.9)	−15.3 (−32.7)	14.5 (7.2)	8.0 (−5.2)
UCCSD(T)/6-31G**	17.3 (9.4)	13.6 (5.2)	15.2 (6.6)	−14.9 (−32.3)	15.6 (8.3)	8.7 (−4.5)
UCCSD(T)/6-311+G**	17.0 (9.1)	13.1 (4.7)	13.8 (5.2)	−17.2 (−34.6)	14.2 (6.9)	6.3 (−6.9)
CASPT2(10,8)/6-31G**	6.7	0.1	2.3	−18.9	4.6	3.3

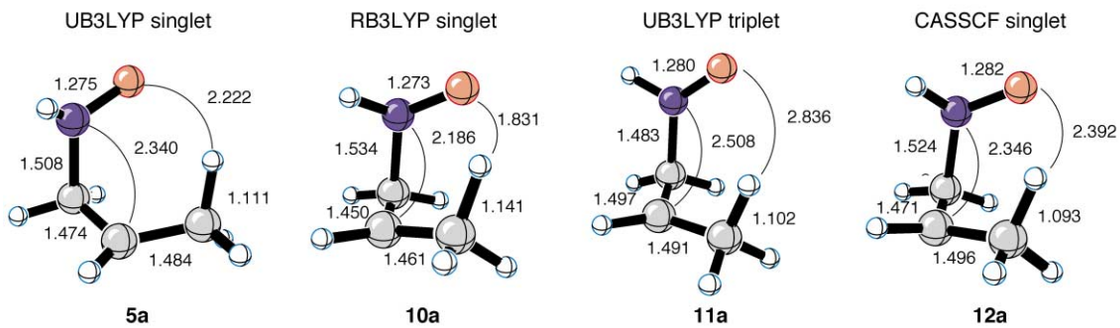

Fig. 6 Structures of the singlet intermediate optimized with RB3LYP/6-31G*, **10a**, a triplet diradical optimized with UB3LYP/6-31G* **11a** and a CASSCF(10,8)/6-31G* optimized intermediate **12a** compared to that of the UB3LYP/6-31G* optimized singlet diradical, **5a**.

diradical – all of which are expected to have important open shell contributions but are considerably in error for the species that are expected to be closed shell – the aziridine *N*-oxide and ene product.

It is known that these ene reactions are facile at room temperature and below. EPR experiments estimated the activation energy for the reaction between PhNO (which should be less reactive than HNO) and TME to be 10 kcal mol^{-1}.[33] The balance of evidence favors energetics like those calculated with B3LYP and CASPT2. Spin projection of the B3LYP energies employing the procedure of Yamaguchi *et al.*[21] lowers the energy of the intermediate and puts it closer to the CASPT2 value. However, the energy is lowered by too much and overshoots and consequently, subsequent discussions will report both corrected and uncorrected energies for the diradicals and these are expected to place upper and lower limits on the correct energy of the pure singlet diradical.

Properties of the intermediate

As indicated above, the open chain intermediate optimized with UB3LYP involves some spin contamination. Optimizations with RB3LYP yielded a very similar structure, **10a** (Fig. 6) which was 1.8 kcal mol^{-1} higher in energy than the UB3LYP structure (7.4 kcal mol^{-1} above the energy after spin projection). A CASPT2(10,8)/6-31G** single point calculation on the RB3LYP structure confirmed that it is indeed higher in energy than the UB3LYP structure, but this method placed the energy difference at only 0.5 kcal mol^{-1}. A triplet diradical, **11a**, could also be optimized and was 5.2 kcal mol^{-1} above the singlet (10.8 kcal mol^{-1} after spin projection in the singlet). Concerns about the effect of the spin contamination by the triplet in UB3LYP prompted an optimization of the intermediate with CASSCF(10,8)/6-31G* calculations. This structure, **12a**, is very similar to the UB3LYP structure, **5a**.

The CASSCF calculations revealed details of the orbitals involved in the diradical intermediate. The two near degenerate orbitals that lead to the existence of diradical type character are a bonding and antibonding combination of the NO π* orbital and the 2p orbital on carbon (Fig. 7). Denoting these two orbitals as ϕ_1 and ϕ_2 respectively, there are three possible singlet descriptions formed from Ψ_1, Ψ_2, Ψ_3 and Ψ_4. A pure closed shell polar structure would be adequately described by either Ψ_1 or Ψ_2, a single reference description. A pure diradical must be

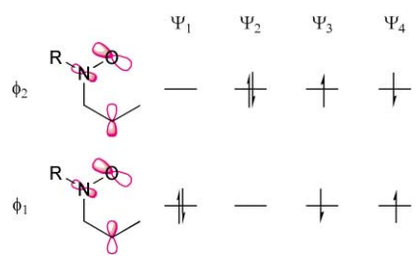

Fig. 7 Four possible electronic configurations for the open chain intermediate involving the two nearly degenerate orbitals ϕ_1 and ϕ_2.

multireference and may be described as $\Psi_1 - \Psi_2$ or $\Psi_3 - \Psi_4$. $\Psi_3 + \Psi_4$ is the $m_S = 0$ component of a triplet diradical.

Our CASPT2 calculations reveal that the optimal wavefunction at the diradical geometry is composed of approximately $0.867\Psi_1 - 0.437\Psi_2$ with small contributions from other configurations. This indicates an approximately 50 : 50 mixture of the diradical ($\Psi_1 - \Psi_2$) and the closed shell polar structure Ψ_1. This hybrid nature of the intermediate suggests that the intermediates be called neither diradicals nor zwitterions, but polarized diradicals. The polar character is emphasized by the NBO atomic charges shown in Fig. 8. These charges show that approximately 0.2 electrons have been transferred to the nitroxyl grouping from the alkene moiety.

In polar solvents, the polar contributions to the electronic structure of the intermediate might be expected to be enhanced

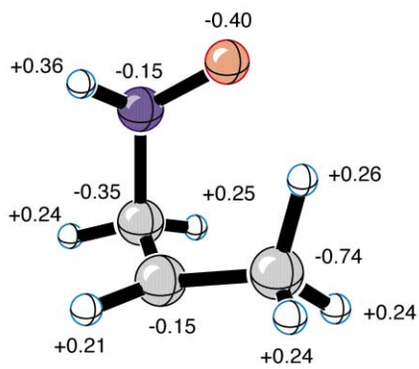

Fig. 8 Atomic charges for the polarized diradical intermediate **5a** calculated with the NBO method.

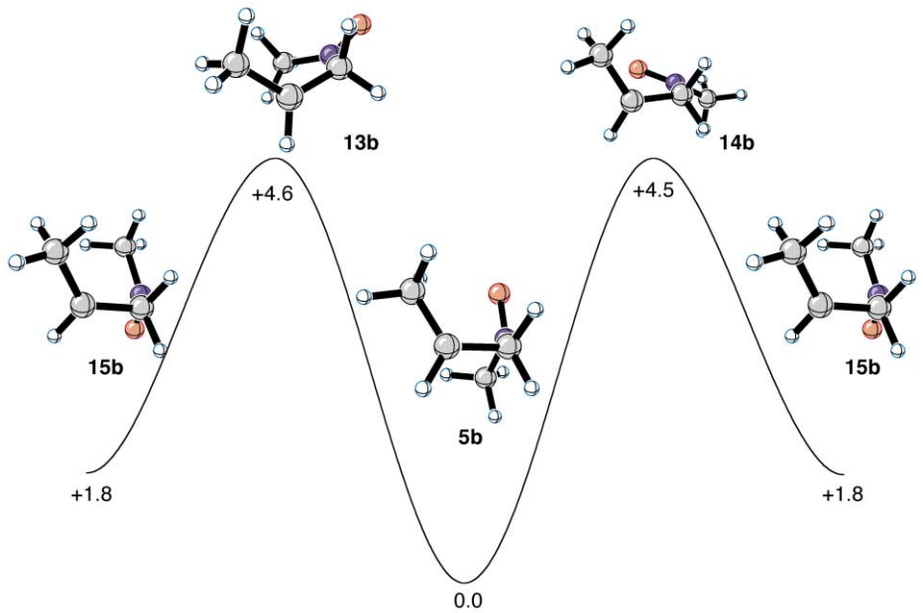

Fig. 9 Profile for rotation about the C1–N bond in polarized diradical **5b**.

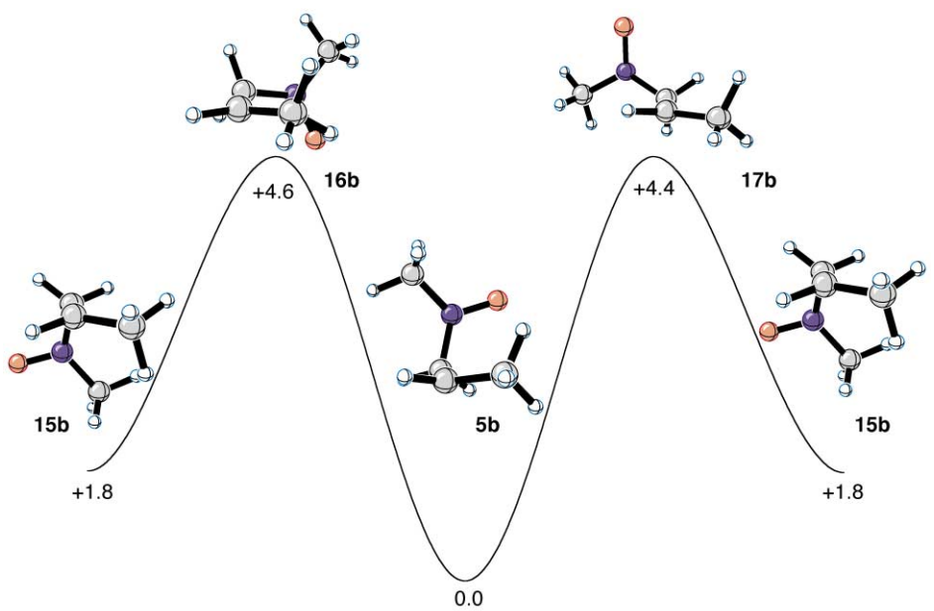

Fig. 10 Profile for rotation about the C1–C2 bond in polarized diradical **5b**.

at the price of decreased diradical character. The polar component should also allow a significant energy lowering of the intermediate. Optimization using the PCM solvent model confirmed this behavior (Table 2). As solvents with increasing dielectric constant are used, the $<S^2>$ value diminishes, indicating a decreasing diradical contribution. The energy also decreases, indicating a stabilization of the polar structure and hence its increased contribution to the electronic structure of the polarized diradical.

The interaction of NO π* and C 2p orbitals naturally leads to a bonding interaction between the carbon and nitrogen atoms. Although this is short of being a full covalent bond, as in the aziridine *N*-oxide, it is expected to restrict rotation in the polarized diradical. This is essential if a formally open chain intermediate is to be consistent with experimental kinetic isotope effects. This has been probed by locating the transition states for rotation in the polarized diradical, **5b**, formed between MeNO and propene. In this polarized diradical, the C–N rotation barriers are 4.6 and 4.5 kcal mol^{-1}, (Fig. 9) corresponding to **13b** and **14b** for the two directions of rotation. These barriers link the polarized diradical to an alternative conformation, **15b**, which is 1.9 kcal mol^{-1} above **5b**. Similarly, rotation about the C_1–C_2 bond is calculated to have barriers of 4.6 and 4.4 kcal mol^{-1} (Fig. 10) corresponding to **16b** and **17b** and leads to the same alternative conformer, **15b**.

Table 2 Energies (kcal mol^{-1}) relative to solvation optimized reactants and $<S^2>$ values for the polarized diradical **5a** optimized using the PCM method to evaluate solvation in three solvents of varying polarity

Solvent	ε_{rel}	E_{rel}	$<S^2>$
None	1.0	1.4	0.64
Chloroform	4.9	0.2	0.59
Ethanol	24.6	−3.3	0.47
Water	78.4	−3.4	0.36

In more substituted examples such as the diradical, **18**, fomed between 2-methylbut-2-ene and MeNO, the barriers to rotation are even higher. The barriers to rotation about the C–N bond

were 5.2 and 6.3 kcal mol^{-1} relative to the twix conformer (discussed in more detail in the section on regioselectivity) and were 4.3 and 5.2 kcal mol^{-1} relative to the higher energy twin conformer. The barrier to rotation about the C1–C2 bond is 6.2 kcal mol^{-1} relative to the twix diradical and 5.7 kcal mol^{-1} relative to the twin conformer.

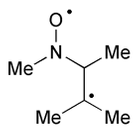

18

Conformer **5b** has the potential to include a CH–O hydrogen bond which might also contribute to these elevated barriers to rotation. To estimate the relative contributions of the CH–O hydrogen bond and the C–N bonding interaction to the rotation barrier, the corresponding barriers in the diradical, **19** (Fig. 11), formed between ethene and MeNO in which the hydrogen bond must be absent but the C–N interaction can remain were calculated. Similarly the radical, **20**, formed by adding hydrogen to the carbon radical in **5b** would maintain the hydrogen bond but lack a C–N interaction.

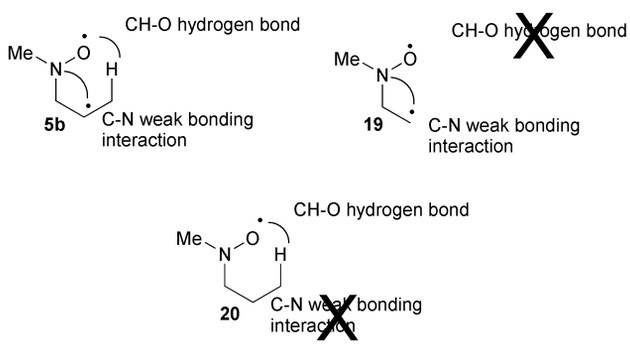

Fig. 11 Model compounds which maintain only one of the two important interactions in **5b** which contribute to elevated barriers to rotation.

In the model diradical **19** which lacks a CH–O hydrogen bond, the barrier to rotation about the C–C bond was found to be 2.5 kcal mol^{-1} (Fig. 12), 2 kcal mol^{-1} less than in the diradical **5b**. The removal of the methyl group may lower the barrier (sterically) by ~1 kcal mol^{-1} itself and so the hydrogen bond may have contributed ~1 kcal mol^{-1} to the C–C rotational barrier heightening in **5b**. Rotation about the C1–N bond in **19** is expected to be affected by the extra methyl group less than the C1–C2 rotation. A barrier of 2.3–2.6 kcal mol^{-1} is calculated for rotation about the C1–N bond (Fig. 13). This is also ~2 kcal mol^{-1} less than the C–N rotation in **5b**. The hydrogen bond may therefore be contributing ~ 2 kcal mol^{-1} to the C–N rotational barrier heightening in **5b**.

In the diradical **20**, which maintains the hydrogen bond but has lost the possibility of C–N interaction, the barrier to rotation about the C1–C2 bond is calculated to be 2.4–4.1 kcal mol^{-1} (Fig. 14). This suggests that the C–N interaction may be contributing 0.5–2 kcal mol^{-1} to the C1–C2 rotational barrier. In the rotational scan about the C1–N bond in **20** (Fig. 15), one very low barrier was found, that in which the CH–O hydrogen bond is maintained, the deformation to achieve rotation is principally an inversion at N which has little cost in these kinds of R_2NO structures.[34] In the rotational transition states where the CH–O hydrogen bond is sacrificed, barriers of 2.6–3.3 kcal mol^{-1} are found. This suggests that the C–N interaction may be contributing 1–2 kcal mol^{-1} to the enhanced rotational barrier in **5b**. Overall, the CH–O hydrogen bond and the weak C–N bonding interaction contribute approximately equally, ~1–2 kcal mol^{-1} to the enhanced rotational barrier.

To understand the existence of a barrier between the azirdine *N*-oxide and the diradical, the process of stretching the CN bond in the aziridine *N*-oxide was analyzed (Fig. 16). Such stretching would produce a diradical in which one unpaired electron is on carbon and one on nitrogen, in a π^* orbital since there is overlap with an O lone-pair orbital. This would be the

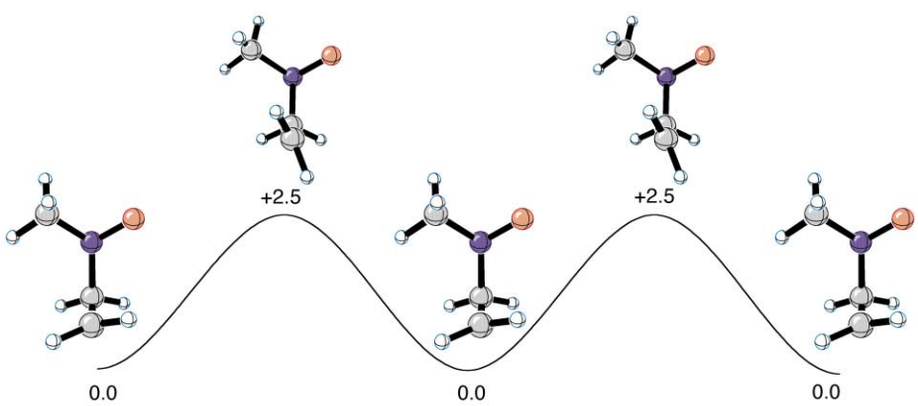

Fig. 12 Profile for rotation about the C1–C2 bond in polarized diradical **19**.

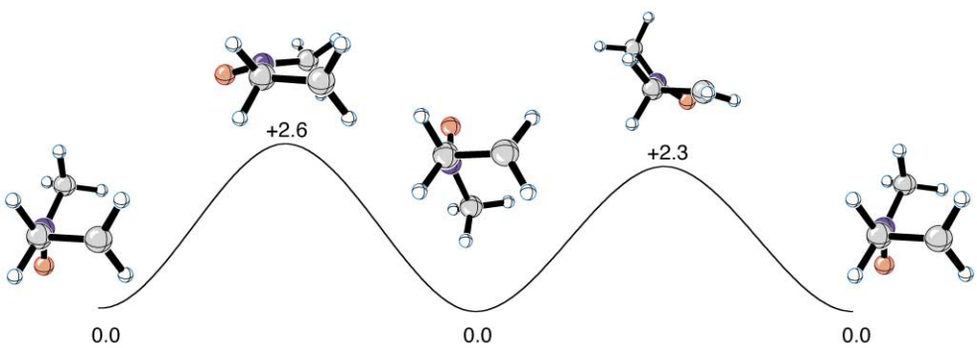

Fig. 13 Profile for rotation about the C1–N bond in polarized diradical **19**.

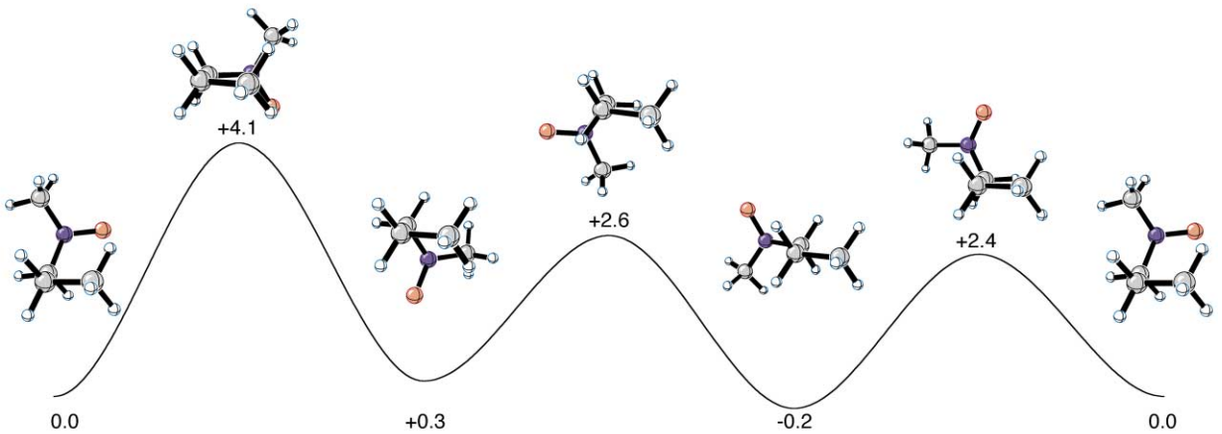

Fig. 14 Profile for rotation about the C1–C2 bond in polarized diradical **20**.

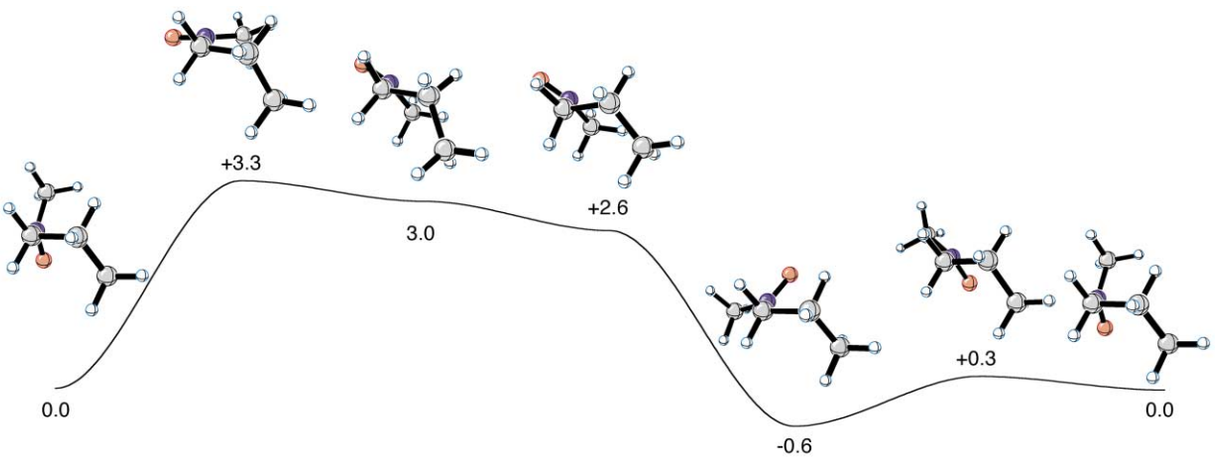

Fig. 15 Profile for rotation about the C1–N bond in polarized diradical **20**.

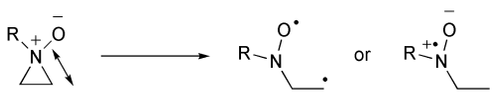

Fig. 16 The possible products of stretching the bond of an aziridine *N*-oxide.

lowest electronic structure of the diradical if the NO π* orbitals were polarized towards N. However, nitrogen is nonplanar and the orbitals are formed by mixing of an sp^3 orbital with an oxygen 2p orbital, which is higher in energy, to form the p and π* orbitals. The isolated nitroxide radical in fact resembles an oxyradical, and hence the known preference for radical quenching at the oxygen atom of radicals such as TEMPO rather than at nitrogen. The orbitals take the form shown in Fig. 17.

Cleavage of the C–N bond of the aziridine *N*-oxide corresponds to initial correlation with the aminyl radical, or essentially the π–π* excited state of the nitroxide radical.[35] This has been calculated to be 6.18 eV higher[35] than the oxyradical ground state for $H_2NO^{\bullet}$ and experimentally measured to be 5.17–5.39 eV higher for substituted examples.[36] The polarized diradical and aziridine *N*-oxide do not have identical electronic structures, and their interconversion corresponds to an initial correlation of ground and excited electronic states. Consequently, a barrier exists between the two species.

Similar polarized diradical species (such as **21**) may be relevant to reactions such as the Paternò–Büchi reaction between excited state carbonyls and alkenes.[37]

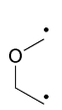

21

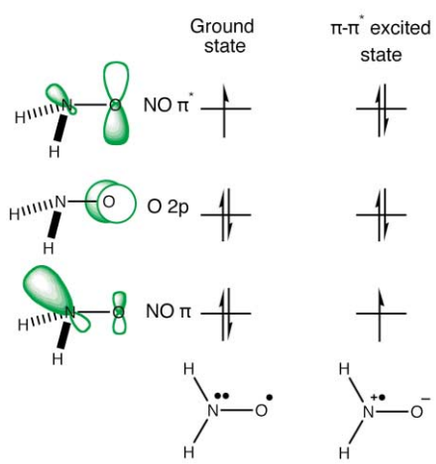

Fig. 17 The frontier orbitals of nitroxides, $R_2NO^{\bullet}$.

Validity of the model reactions

The experimental data that are available for these reactions generally involve reactions of electron-deficient nitrosoarenes. Due to the computational expense of study of such systems, HNO or MeNO were employed as models. In order to determine whether the results for the model system translate to the experimental systems, the reactions of propene with HNO, MeNO and *p*-$NO_2C_6H_4NO$ were studied as well. All were found to follow the same mechanism already described for HNO, involving the intermediacy of a polarized diradical.

The energetics for the three reactions are listed in Table 3, and the structures for the MeNO and *p*-$NO_2C_6H_4NO$ reactions are shown in Schemes 4 and 5, respectively. These clearly show

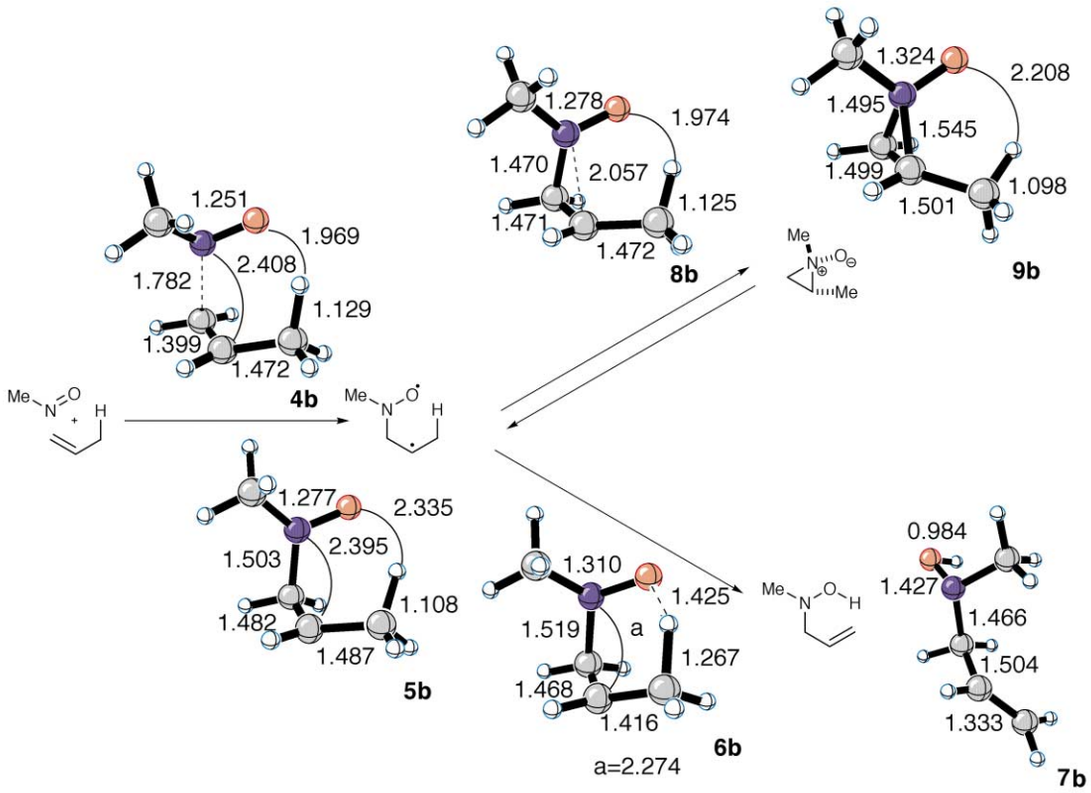

Scheme 4 The B3LYP/6-31G* mechanism for the reaction between MeNO and propene.

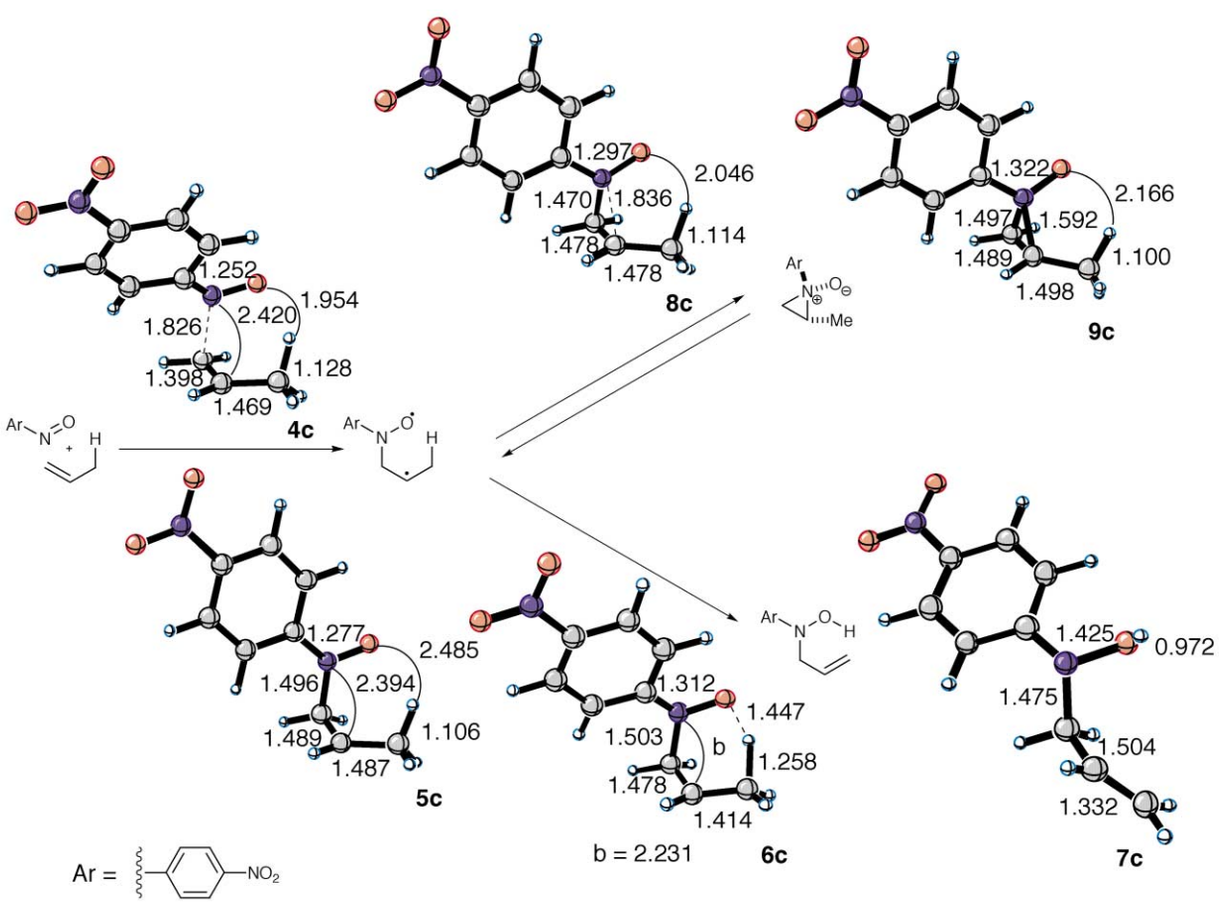

Scheme 5 The B3LYP/6-31G* mechanism for the reaction between *p*-$NO_2C_6H_4NO$ and propene.

that while HNO has very low barriers, presumably reflecting its high electrophilicity, MeNO and *p*-$NO_2C_6H_4NO$ show energetics and geometries which are very similar. The one exception to this is that when corrections to the electronic energy are included to produce enthalpies, the aziridine *N*-oxide and the transition state linking it to the diradical are equienergetic for

Table 3 UB3LYP/6-31G* energetics for the reaction of HNO, MeNO and *p*-$NO_2C_6H_4NO$ with propene. Spin projected energies are in parentheses. Enthalpies are presented in kcal mol^{-1}

RNO		4	5	6	7	8	9
HNO	**a**	6.4	3.7 (−1.9)	4.8	−14.7	6.8	3.9
MeNO	**b**	14.3	9.7 (5.1)	12.9	−10.3	12.5 (11.7)	7.7
p-$NO_2C_6H_4NO$	**c**	14.4	7.7 (4.5)	10.8	−12.4	11.8	11.8

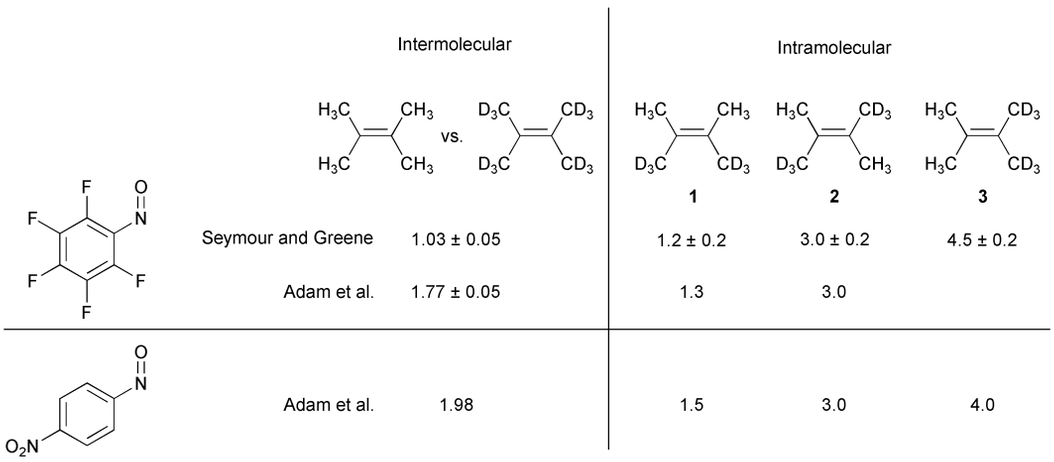

Fig. 18 Summary of experimentally measured kinetic isotope effects for the reaction between nitrosoarenes and isotopically labeled tetramethylethylenes (TME).

the nitrosoarene. One key cause of this behavior is that in all species apart from the aziridine *N*-oxide and the reactants, the nitrogen lone pair overlaps to a greater or lesser extent with the aromatic ring. In the aziridine *N*-oxide and reactants, this lone pair is orthogonal to the aromatic system. A similar effect is observed for the reaction of nitrosoethylene: the aziridine *N*-oxide is only 0.4 kcal mol^{-1} lower in enthalpy than the transition state linking it to the polarized diradical (Scheme 6), in contrast to the differences of 2.9 and 4.8 kcal mol^{-1} calculated for HNO and MeNO, respectively.

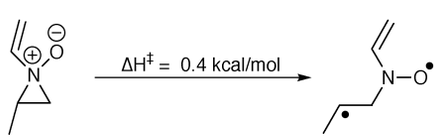

Scheme 6 The activation enthalpy for the ring-opening of the aziridine *N*-oxide formed between nitrosoethene and propene.

Further evidence for the validity of MeNO as a model for the nitrosoarenes comes from the good agreement found between calculations using this model and experimental kinetic isotope effects and regioselectivities detailed below.

Kinetic isotope effects

Seymour and Greene measured the kinetic isotope effects for deuterated isomers of TME reacting with C_6F_5NO.[12] These show a small (secondary) isotope effect (k_H/k_D = 1.03) for the intermolecular competition between d_{12}-TME and d_0-TME. This suggests a rate limiting step which does not involve hydrogen abstraction. A similar small secondary isotope effect is seen for the isotopomer **1** which presents only CH_3 or CD_3 groups on each side of the alkene. This suggests that the selectivity determining step does not allow selection between the two sides of the alkene. By contrast, the two isotopomers, **2** and **3**, which have a CH_3 and CD_3 group on each side of the alkene show primary isotope effects (k_H/k_D = 3.0 for **2** and k_H/k_D = 4.5 for **3**). This suggests that the selectivity determining step allows selection between the two ends of the alkene. They concluded that these isotope effects are consistent with the intermediacy of an aziridine *N*-oxide or a mechanism having similar features.

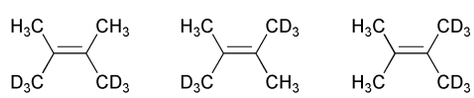

Adam *et al.* recently remeasured the isotope effects and found a different value for the intermolecular isotope effect.[13] They speculated that the highly reactive nature of the nitroso enophiles may cause local depletion of the nitroso compound and different isotope effects to be measured. They performed the measurements with low concentrations and conversions and found a value of k_H/k_D = 1.77. They also repeated the experiments using *p*-$NO_2C_6H_4NO$ as enophile. All of these values are shown in Fig. 18. When KIEs such as these have been observed in ene reactions of other enophiles, notably triazolinediones, most authors have used them to rule out diradicals (or zwitterions) as possible intermediates because they expected the open chain nature of such species was expected to allow rapid rotation which should give primary KIEs for *cis*- and *trans*-d_6-TME but secondary KIEs for *gem*-d_6-TME. Rotation barriers in these open chain intermediates are calculated to be larger than those for H abstraction and for closure to an aziridine *N*-oxide, thus enabling such intermediates to be consistent with the experimental observations.

The program QUIVER was used to calculate KIEs, using B3LYP/6-31G* frequencies.[29] In those cases for which the KIE determining step does not involve hydrogen abstraction, the Bell correction for tunneling was applied.[30] The reaction between MeNO and TME was employed as a theoretical model and the calculated energetics are summarized in Scheme 7. This reaction is computed to form the polarized diradical **5d** in a fairly reversible fashion and decomposition is equally likely as cyclization to the aziridine *N*-oxide **9d**. The barrier to ene product formation from the polarized diradical is higher by 0.7 kcal mol^{-1}. In most of the reactions described in this paper, hydrogen abstraction is calculated to be more favorable than cyclization to form the aziridine *N*-oxide and the initial polarized diradical formation is the highest point on the reaction profile. This mirrors the significantly decreased exothermicity of the ene reaction in this case.

For the intermolecular isotope effects (d_0 *versus* d_{12}), there are two limiting calculated values (Fig. 19). If the formation of

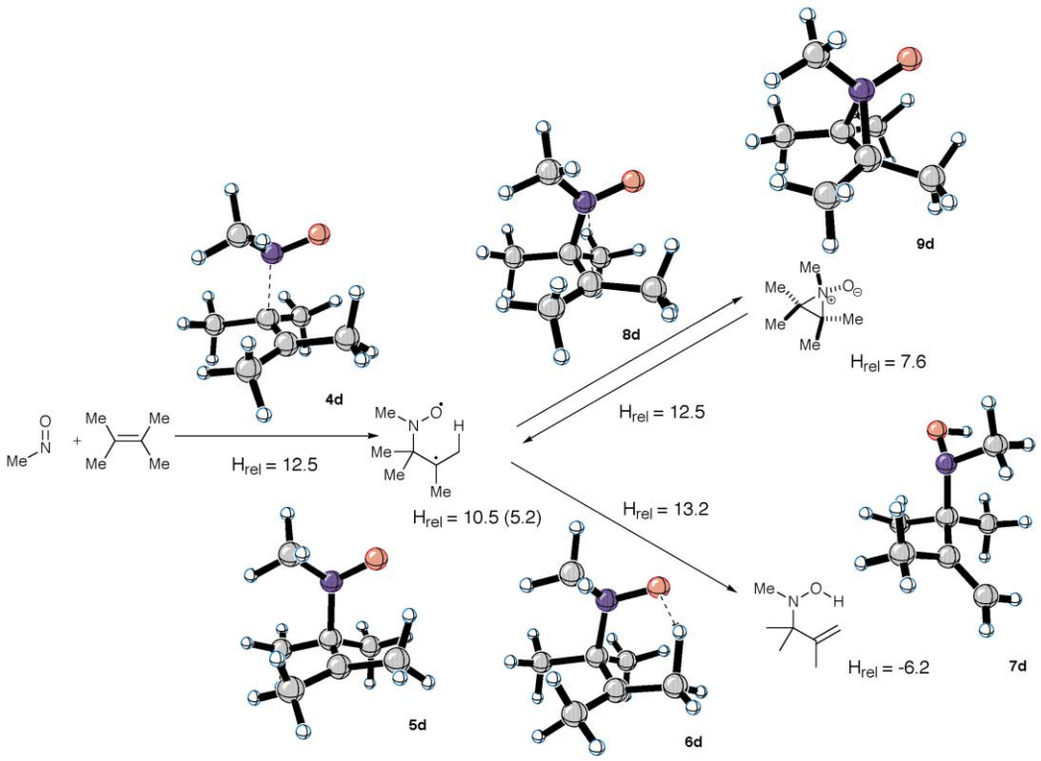

Scheme 7 The B3LYP/6-31G* mechanism for the reaction between MeNO and TME.

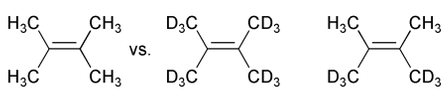

Irreversible	1.12	1.14
Reversible	3.56	4.13

Fig. 19 Summary of calculated kinetic isotope effects based on two limiting assumptions : (1) completely irreversible formation of a polarized diradical, **5d**, and (2) completely reversible formation of **5d**.

polarized diradicals is assumed to be completely irreversible, a secondary isotope effect of k_H/k_D = 1.12 for the first step is expected because an irreversibly formed diradical could only abstract hydrogen if it was formed from the d_0 isotopomer and only abstract deuterium if it was formed from the d_{12} isotopomer. However, if the formation of polarized diradical is completely reversible, then the selection between reactant with 12 protons or 12 deuterons is only made when one of these isotopes is abstracted in the ene product forming step. The upper limit for the intermolecular kinetic isotope effect would therefore be a primary one, with k_H/k_D = 3.56 being calculated when the equilibrium isotope effect on polarized diradical formation was included.

If it is assumed 1) that the computed isotope effects are correct for each process and 2) that the experimental isotope effect reflects a partitioning between the reactants that undergo reversible polarized diradical formation and those that undergo hydrogen abstraction upon diradical formation, the fraction of polarized diradicals that undergoes each process can be calculated. Using Adam's value for F_5C_6NO of 1.77, 74% of polarized diradicals should directly undergo ene reaction without reversion to reactants whereas 26% should undergo reversion. Hydrogen abstraction should have a barrier that is lower than that for reversion by 0.5 kcal mol^{-1}. For the value measured for *p*-$NO_2C_6H_4NO$, 65% of polarized diradicals should directly abstract hydrogen and 35% revert to reactants. This corresponds to a difference in barrier heights of 0.3 kcal mol^{-1}. The calculated barriers are ordered differently and show that reversion should be more facile than hydrogen abstraction by 0.7 kcal mol^{-1}. Employing the difference in barrier heights obtained with B3LYP, an intermolecular kinetic isotope effect of k_H/k_D = 3.00 is calculated.

Similar arguments may be applied to the reaction of *cis*-d_6-TME, **1**. Calculations described earlier suggest that rotation in the polarized diradical is not expected to be competitive with any of the bond forming or breaking processes. Any polarized diradical that proceeds to hydrogen abstraction rather than reverting to reactants will only be able to abstract one kind of isotope which will be governed by whether the diradical is formed with the NO group directed towards the side of the alkene with two CH_3 or two CD_3 groups. The KIE of k_H/k_D = 1.14 calculated for the first step for *cis*-d_6-TME, would be appropriate for no reversibility (Fig. 19). The kinetic isotope for the second step, hydrogen abstraction, which would be appropriate for complete reversibility is k_H/k_D = 4.13. To be consistent with experiment, these values require 95% of polarized diradicals to directly undergo hydrogen abstraction rather than reverting to reactants. The barrier to hydrogen abstraction should therefore be lower than that for reversion by 1.5 kcal mol^{-1}; in contrast to the calculated difference of 0.7 kcal mol^{-1} in the wrong direction.

In the two cases of *trans*-d_6-TME, **2**, and *gem*-d_6-TME, **3**, the intramolecular isotope effects are governed by processes subsequent to formation of the polarized diradical and so the reversibility of this process will only affect the isotope effects by a small equilibrium effect which has not been computed. Two isotope effects are calculated for these two isotopomers. A secondary isotope effect, corresponding to the reactions in which the polarized diradical forms and then directly abstracts whichever isotope is positioned to be abstracted. This is determined by the structure of the diradical formed in the first step, which does not involve hydrogen abstraction. A larger primary isotope effect is also possible: if the diradical cyclizes to an aziridine *N*-oxide before hydrogen abstraction, it may then reopen to either the original diradical or to the isomer in which the NO fragment has become attached to the other end of the alkene. In this way, selection between the two ends of the alkene is possible and the KIE corresponding to the hydrogen abstraction step would result. The KIEs expected for these two extremes are indicated in Fig. 20.

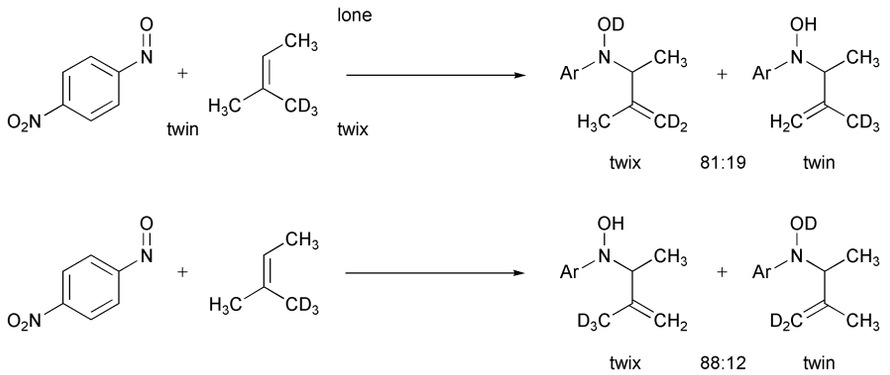

Scheme 8 Experimentally observed regioselectivity for isotopically labeled isomers of 2-methylbut-2-ene.[8]

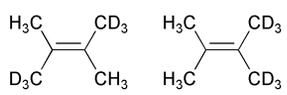

Direct hydrogen abstraction	1.19	1.53
Cyclization to ANO	4.20	5.32

Fig. 20 Summary of kinetic isotope effects calculated based on two limiting assumptions: (1) polarized diradicals undergo exclusive hydrogen abstraction; (2) polarized diradicals undergo cyclization to an aziridine *N*-oxide before undergoing hydrogen abstraction.

The mechanism that was calculated for the reaction was one in which these two extremes of mechanism are energetically close and therefore in competition. In line with this, the two calculated values delimit a range that include the experimental value. If it is assumed that the calculated values are correct for each of the two possible mechanisms, they can be used to estimate the fraction of reactions which should proceed through the two possible mechanisms, as outlined above for the intermolecular isotope effects. Thus, in the case of *trans*-d_6-TME, 40% should proceed through direct abstraction and for *gem*-d_6-TME, 22%. These partitionings between the two mechanisms correspond to differences in barrier heights of 0.2 and 0.7 kcal mol^{-1}, with the barrier to cyclization expected to be lower than that for hydrogen abstraction. The B3LYP calculated value is 0.7 kcal mol^{-1}.

Considering the complexity of the mechanistic situation, all of the calculated values are in remarkably good agreement with the experimental values (which were measured with a different nitroso compound than used for the calculations). The intermolecular isotope effects suggest that the transition state for the initial diradical formation should be higher in energy than has been calculated by 1–2 kcal mol^{-1}, this may be a consequence of using MeNO to model the reactions of nitrosoarenes and follows the trend seen in the model reaction with propene (Table 3).

Regioselectivity

Adam *et al.* have shown that for the reaction of electron poor nitrosoarenes there is a significant preference for abstraction from the allylic position that is at both the most highly substituted side of the alkene and the most substituted end.[8] He adopted a nomenclature to describe this regioselectivity, labeling the allylic positions of 2-methylbut-2-ene as lone, twix and twin. The position of preferred abstraction is twix (Scheme 8). This was exemplified by measuring the regioselectivity in deuterated isomers of 2-methylbut-2-ene. These studies show an approximately 85 : 15 preference for twix abstraction over twin, corresponding to a difference of approximately 0.9 kcal mol^{-1} in the barriers for the two reactions.

The reaction of 2-methylbut-2-ene with both HNO and MeNO was studied. In all cases, the polarized diradical mechanism was found. The relative barriers are presented graphically in Scheme 9 for the reaction of MeNO, which will be discussed first and the corresponding data for the reaction of HNO in Scheme 10.

It is clear that at each step of the reaction the twix path is lowest in energy. It is therefore not surprising that this should be the major product. From the data presented in Scheme 8, the regioselectivity determining step can be identified.

There are three diradicals that can feasibly form. If the twix diradical is formed in the first step (the most likely outcome), it may either directly abstract hydrogen to yield the twix product or (through a transition state at the same energy) may cyclize to form an aziridine *N*-oxide. This aziridine *N*-oxide overlaps with the path for the lone diradical. The barrier to reopening to the twix diradical is lower than that to reopen to the lone diradical but only by 1 kcal mol^{-1}. More significantly, formation of the lone diradical presents a substantially higher barrier to hydrogen abstraction to form the lone product. This diradical will therefore preferentially cyclize to the aziridine *N*-oxide and reopen to form the twix diradical and hence twix product. Alternatively, if the lone diradical is formed directly in the first step, it will also face the same preference and ultimately will yield twix product and not lone. This explains why no abstraction from the lone position is observed. However, if twin diradical is formed in the first step, it has a small preference to undergo hydrogen abstraction to form the twin product. Even if it cyclizes to form the aziridine *N*-oxide, this can only undergo ene reaction by reopening to reform the twin diradical.

The outcome of the first step governs the regioselectivity of the reaction. Any twix or lone diradical that forms will yield twix product. Any twin diradical will yield twin product. Little reversibility of diradical formation has been assumed, as suggested by the kinetic isotope effects discussed earlier. Our calculations allow us to predict a twix : twin ratio of 76 : 24. Of the fraction forming twix product, 71% will have arisen from initially formed twix diradical and 5% from initially formed lone diradical. This ratio is in excellent agreement with the experimental ratio.

The cause of this regioselectivity, can be seen in the twix and twin transition states for polarized diradical formation. These are the key transition states determining the product mixture. In Fig. 21, key distances are shown that relate to potential steric clashes shown with the jagged line and potential electrostatically favorable CH–O interactions are shown with the curves. The twix approach benefits from two favorable CH–O interactions and suffers only one small interatomic approach (steric repulsion) whereas the "twin" approach has only one beneficial CH–O interaction but suffers from two near approaches. The effects illustrated in Fig. 21 are also the key contributors to the more general "*cis*-effect" observed for the reactions of singlet oxygen where a significant preference for hydrogen abstraction from the more substituted side of a double bond is observed.[38]

A different regioselectivity is calculated for the reaction of HNO, as shown in Scheme 9. This occurs because HNO is less

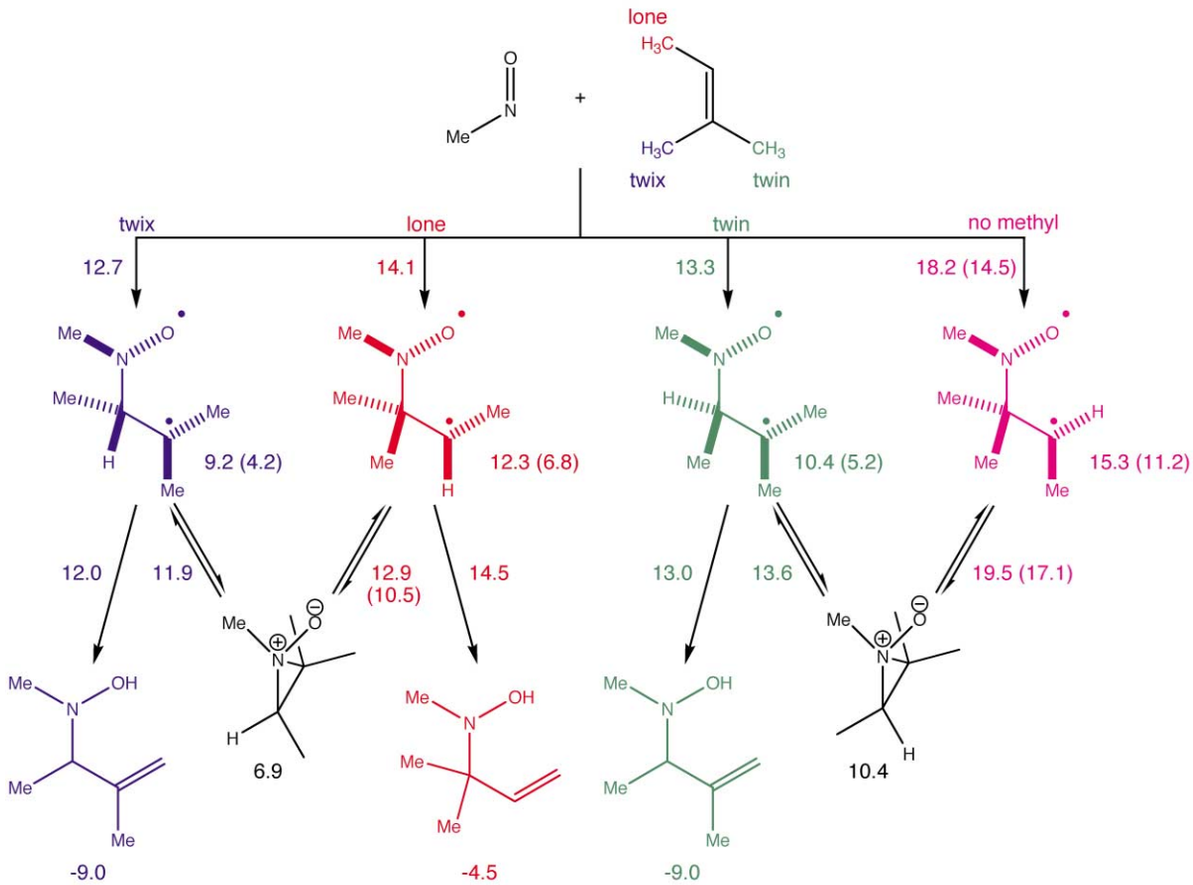

Scheme 9 Schematic showing B3LYP/6-31G* energetics for the ene reaction between MeNO and 2-methylbut-2-ene.

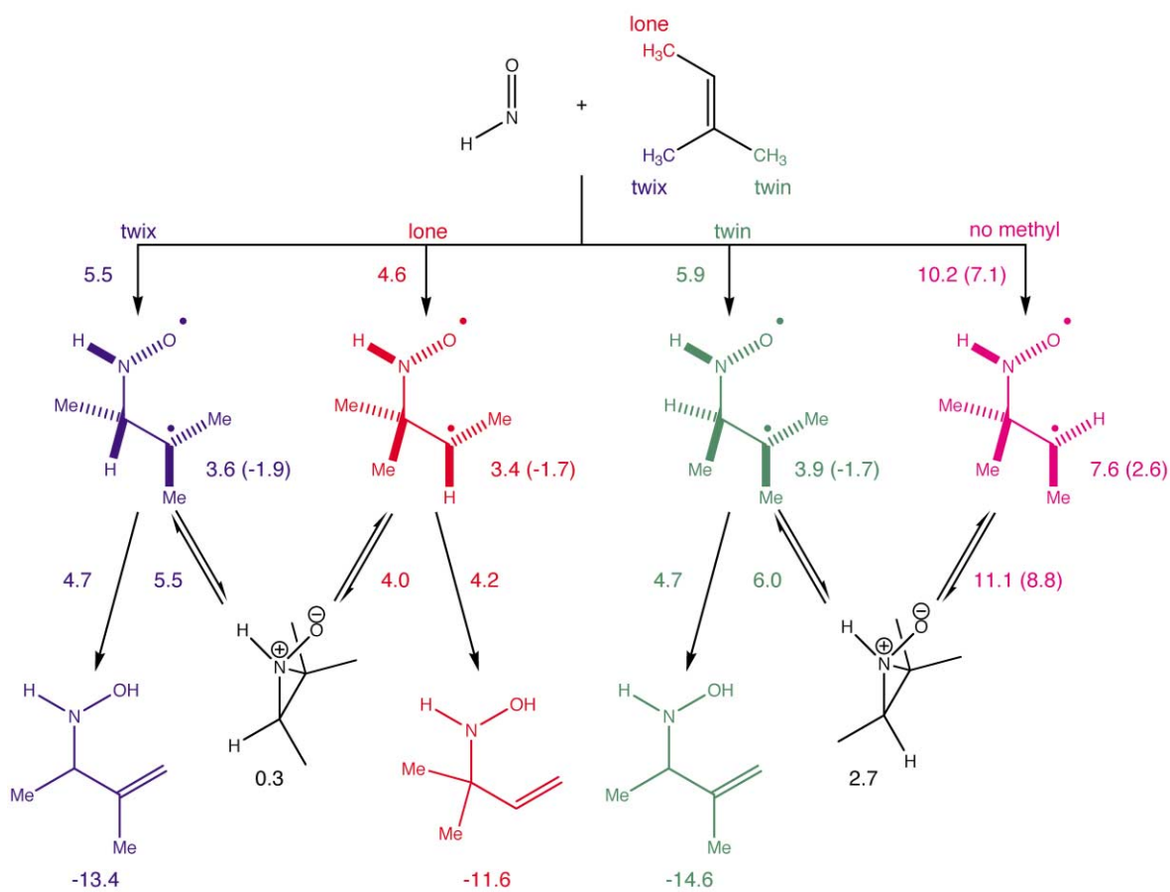

Scheme 10 Schematic showing B3LYP/6-31G* energetics for the ene reaction between HNO and 2-methylbut-2-ene.

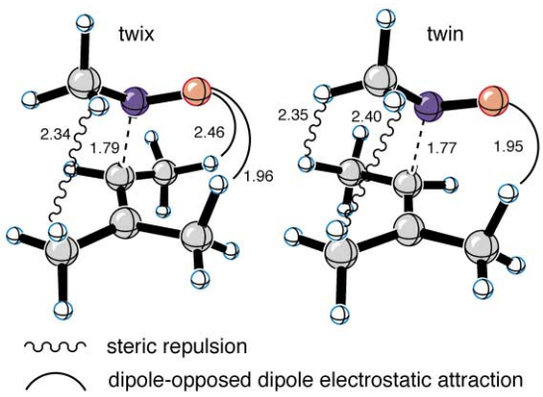

Fig. 21 The origin of the selectivity for twix over twin.

sterically demanding in nature and is more electrophilic. This would be expected to make it more like singlet oxygen in reactivity. Polarized diradical formation is still calculated to occur. This polarized diradical still has a preference for cyclization to an aziridine *N*-oxide compared to hydrogen abstraction, but this is small and the aziridine *N*-oxide has a preference to reopen to form lone diradical. Therefore, lone diradical formed on the first step should lead principally to lone product, twix diradical to twix product and twin diradical to twin product. A twix : twin : lone ratio of 17 : 8 : 75 is predicted. This resembles the case of singlet oxygen where the ratio of 36 : 7 : 57 is observed (averaged over the two analogous isotopically labeled species shown in Scheme 7). However, the mechanism of the ene reaction of singlet oxygen is significantly different from that for nitroso compounds.[39] The reaction of singlet oxygen involves a two step no intermediate mechanism in which an initial transition state leads to a second transition state rather than a minimum. A reaction path bifurcation intervenes between the two transition states and the outcome is therefore governed dynamically. The underlying causes of regioselectivity are presumably similar despite the different mechanisms.

Conclusions

The ene reactions of nitroso compounds involve the intermediacy of polarized diradicals. This species has an electronic structure between that of a closed shell, polar structure and that of a pure diradical. A weak but significant interaction between the nitrogen atom and the carbon centered radical as well as a CH–O hydrogen bond lead to larger than expected barriers to rotation about formal single bonds in the polarized diradical intermediate. The aziridine *N*-oxide is formed as a bystander, and although not a compulsory intermediate for the reaction does permit translation of the RNO fragment from one end of the alkene to the other.

B3LYP/6-31G* provides energetics that are in good agreement with those of higher level methods for this reaction. Constrained optimizations permit the clear visualization of the potential energy surface for the reaction and demonstrate that the lowest energy path for the reaction passes through an open chain intermediate. The polarized diradical intermediates can be optimized with both restricted and unrestricted calculations.

At first sight the experimentally observed kinetic isotope effects seem to rule out the possible involvement of open chain species. However, the high barriers to rotation in the polarized diradicals prevent the stereochemical scrambling usually associated with open chain species. Kinetic isotope effects can be calculated using the data from frequency calculations on the various transition states and minima. These are consistent with the experimentally observed values and require that the formation of aziridine *N*-oxide be reversible to a certain degree and that polarized diradicals partition into two groups one of which directly abstracts hydrogen while the other cyclizes to form aziridine *N*-oxide.

The regioselectivity of the reaction of nitrosoarenes can be modeled satisfactorily using MeNO as the nitroso component, while HNO is predicted to resemble singlet oxygen regioselectivity more closely.

Acknowledgements

We are grateful to the UK Fulbright Commission and AstraZeneca (for a fellowship to AGL) and to the National Science Foundation and National Computational Science Alliance for support. We warmly acknowledge Professor W. Adam for stimulating communications and for sharing results prior to publication.

References

1 A. G. Leach and K. N. Houk, *Chem. Commun.*, 2002, 1243–1255.
2 K. N. Houk, J. C. Williams Jr., P. A. Mitchell and K. Yamaguchi, *J. Am. Chem. Soc.*, 1981, **103**, 949–951.
3 (*a*) G. W. Kirby, *Chem. Soc. Rev.*, 1977, **6**, 1; (*b*) N. E. Jenkis, R. W. Ware Jr., R. N. Atkinson and S. B. King, *Synth. Commun.*, 2000, **30**, 947; (*c*) M. H. Davery, V. Y. Lee, R. D. Miller and T. J. Marks, *J. Org. Chem.*, 1999, **64**, 4976; (*d*) W. W. Wood and J. A. Wilkin, *Synth. Commun.*, 1992, **22**, 1683; (*e*) P. Quadrelli, A. G. Invernizzi and P. Caramella, *Tetrahedron Lett.*, 1996, **37**, 1909; (*f*) S. F. Martin, M. Hartmann and J. A. Josey, *Tetrahedron Lett.*, 1992, **33**, 3583.
4 (*a*) S. Iwasa, K. Tajima, S. Tsushima and H. Nishiyama, *Tetrahedron Lett.*, 2001, **42**, 5897–5899; (*b*) H. E. Ensley and S. Mahadevan, *Tetrahedron Lett.*, 1989, **30**, 3255–3258.
5 (*a*) D. J. Dixon, S. V. Ley and D. J. Reynolds, *Angew. Chem., Int. Ed.*, 2000, **39**, 3622; (*b*) I. Cabanal-Duvillard, J.-F. Berrien, L. Ghosez, H.-P. Husson and J. Royer, *Tetrahedron*, 2000, **56**, 3763; (*c*) I. Cabanal-Duvillard, J.-F. Berrien and J. Royer, *Tetrahedron: Asymmetry*, 2000, **11**, 2525; (*d*) M. J. Wanner and G.-J. Koomen, *J. Chem. Soc., Perkin Trans. 1*, 2001, 1908–1915.
6 W. Adam and N. Bottke, *J. Am. Chem. Soc.*, 2000, **122**, 9846–9847.
7 (*a*) R. E. Banks, R. N. Haszeldine and P. J. Miller, *Tetrahedron Lett.*, 1970, **50**, 4417–4418; (*b*) H. Braun, H. Felber, G. Kreße, A. Ritter, F. P. Schmidtchen and A. Schneider, *Tetrahedron Lett.*, 1991, **47**, 3313–3328; (*c*) J. E. T. Corrie, G. W. Kirby and J. W. M. Mackinnon, *J. Chem. Soc., Perkin Trans. 1*, 1985, 883–886; (*d*) G. W. Kirby, H. McGuigan and D. J. McLean, *J. Chem. Soc., Perkin Trans. 1*, 1985, 1961–1966; (*e*) P. Quadrelli, G. Campari, M. Mella and P. Caramella, *Tetrahedron Lett.*, 1998, **39**, 3233–3236; (*f*) P. Quadrelli, M. Mella and P. Caramella, *Tetrahedron Lett.*, 1998, **39**, 3233–3236; (*g*) W. Adam, N. Bottke, O. Krebs and C. R. Saha-Möller, *Eur. J. Org. Chem.*, 1999, **64**, 1963–1965.
8 W. Adam, N. Bottke and O. Krebs, *J. Am. Chem. Soc.*, 2000, **122**, 6791–6792.
9 (*a*) W. Adam, H.-G. Degen, O. Krebs and C. R. Saha-Möller, *J. Am. Chem. Soc.*, 2002, **124**, 12938–12939; (*b*) W. Adam, K. Peters, E.-M. Peters and S. B. Schambony, *J. Am. Chem. Soc.*, 2001, **123**, 7228–7232; (*c*) F. Sevin and M. L. McKee, *J. Am. Chem. Soc.*, 2001, **123**, 4591–4600; (*d*) E. L. Clennan, *Tetrahedron*, 2000, **56**, 9151–9179; (*e*) G. Vassilikogiannakis, Y. Elemes and M. Orfanopoulos, *J. Am. Chem. Soc.*, 2000, **122**, 9540–9541; (*f*) W. Adam, K. Peters, E.-M. Peters and S. B. Schambony, *J. Am. Chem. Soc.*, 2000, **122**, 7610–7611; (*g*) G. Vassilikogiannakis, M. Stratakis and M. Orfanopoulos, *Org. Lett.*, 2000, **2**, 2245–2248; (*h*) W. Adam, A. Pastor and T. Wirth, *Org. Lett.*, 2000, **2**, 1295–1297; (*i*) M. Stratakis and M. Orfanopoulos, *Tetrahedron*, 2000, **56**, 1595–1615; (*j*) D. A. Singleton and C. Hang, *J. Am. Chem. Soc.*, 1999, **121**, 11885–11893.
10 (*a*) R. G. Parr, L. v. Szentpály and S. Liu, *J. Am. Chem. Soc.*, 1999, **121**, 1922–1924; (*b*) L. R. Domingo, M. J. Aurell, P. Perez and R. Contreras, *J. Phys. Chem. A*, 2002, **106**, 6871–6875; (*c*) L. R. Domingo, M. J. Aurell, P. Perez and R. Contreras, *Tetrahedron*, 2002, **58**, 4417–4423.
11 A. G. Davies and C. H. Schiesser, *Tetrahedron*, 1991, **47**, 1707–1726.
12 C. A. Seymour and F. D. Greene, *J. Org. Chem.*, 1982, **47**, 5227–5229.
13 W. Adam, personal communication.
14 W. Adam, N. Bottke, B. Engels and O. Krebs, *J. Am. Chem. Soc.*, 2001, **123**, 5542–5548.

15 (*a*) M. A. McCarrick, Y.-D. Wu and K. N. Houk, *J. Am. Chem. Soc.*, 1992, **114**, 1499–1500; (*b*) M. A. McCarrick, Y.-D. Wu and K. N. Houk, *J. Org. Chem.*, 1993, **58**, 3330–3343.
16 A. G. Leach and K. N. Houk, *J. Org. Chem.*, 2001, **66**, 5192–5200.
17 (*a*) M. D. Bartberger, J. M. Fukuto and K. N. Houk, *Proc. Natl. Acad. Sci. USA*, 2001, **98**, 2194–2198; (*b*) M. D. Bartberger, W. Liu, E. Ford, K. M. Miranda, C. Switzer, J. M. Fukuto, P. J. Farmer, D. A. Wink and K. N. Houk, *Proc. Natl. Acad. Sci. USA*, 2002, **99**, 10958–10963.
18 Gaussian 98 (Revision A.7), M. J. Frisch, G. W. Trucks, H. B. Schlegel, G. E. Scuseria, M. A. Robb, J. R. Cheeseman, V. G. Zakrzewski, J. A. Montgomery, R. E. Stratmann, J. C. Burant, S. Dapprich, J. M. Millam, A. D. Daniels, K. N. Kudin, M. C. Strain, O. Farkas, J. Tomasi, V. Barone, M. Cossi, R. Cammi, B. Mennucci, C. Pomelli, C. Adamo, S. Clifford, J. Ochterski, G. A. Petersson, P. Y. Ayala, Q. Cui, K. Morokuma, D. K. Malick, A. D. Rabuck, K. Raghavachari, J. B. Foresman, J. Cioslowski, J. V. Ortiz, B. B. Stefanov, G. Liu, A. Liashenko, P. Piskorz, I. Komaromi, R. Gomperts, R. L. Martin, D. J. Fox, T. Keith, M. A. Al-Laham, C. Y. Peng, A. Nanayakkara, C. Gonzalez, M. Challacombe, P. M. W. Gill, B. G. Johnson, W. Chen, M. W. Wong, J. L. Andres, M. Head-Gordon, E. S. Replogle and J. A. Pople, Gaussian, Inc., Pittsburgh PA, 1998.
19 A. D. Becke, *J. Chem. Phys.*, 1993, **98**, 5648–5652.
20 C. Lee, W. Yang and R. G. Parr, *Phys. Rev. B*, 1988, **37**, 785–789.
21 K. Yamaguchi, F. Jensen, A. Dorigo and K. N. Houk, *Chem. Phys. Lett.*, 1988, **149**, 537–542.
22 (*a*) E. Kraka and D. Cremer, *J. Comp. Chem.*, 2001, **22**, 216–229; (*b*) V. N. Staroverov and E. R. Davidson, *J. Am. Chem. Soc.*, 2000, **122**, 186–187.
23 A. G. Leach, S. Catak and K. N. Houk, *Chem. Eur. J.*, 2002, 1290–1299.
24 NBO Version 3.1, E. D. Glendening, A. E. Reed, J. E. Carpenter and F. Weinhold.
25 For the assumed active space (10 electrons in 8 orbitals) which would include 3 otherwise virtual orbitals, $<S^2> = \Sigma (1-(1-p_i)^2)$, where p_i is the population of one of the 3 lowest energy virtual orbitals less the average population of the remaining virtual orbitals. H. Isobe, Y. Takano, Y. Kitagawa, T. Kawakami, S. Yamanaka, K. Yamaguchi and K. N. Houk, *Mol. Phys.*, 2002, **100**, 717–727.
26 MOLCAS Version 5, K. Andersson, M. Barysz, A. Bernhardsson, M. R. A. Blomberg, D. L. Cooper, T. Fleig, M. P. Fülscher, C. de Graaf, B. A. Hess, G. Karlström, R. Lindh, P.-Å. Malmqvist, P. Neogrády, J. Olsen, B. O. Roos, A. J. Sadlej, M. Schütz, B. Schimmelpfennig, L. Seijo, L. Serrano-Andrés, P. E. M. Siegbahn, J. Stålring, T. Thorsteinsson, V. Veryazov, P.-O. Widmark, Lund University, Sweden, 2000.
27 M. Cossi, V. Barone, R. Cammi and J. Tomasi, *Chem. Phys. Lett.*, 1996, **255**, 327.
28 M. W. Wong, *Chem. Phys. Lett.*, 1996, **256**, 391–399.
29 M. Saunders, K. E. Laidig and M. Wolfsberg, *J. Am. Chem. Soc.*, 1989, **111**, 8989.
30 This model multiplies the predicted KIEs by a tunneling correction, B, where $B = u_H\sin(u_D/2)/[u_D\sin(u_H/2)]$, and $u_X = h\nu^{\ddagger}_X/kT$. $\nu^{\ddagger}_X$ is the imaginary frequency for the transition state involving isotope X. (*a*) R. P. Bell, in *The Tunnel Effect in Chemistry*; Chapman and Hall, London, 1980, pp. 60–63; (*b*) R. P. Bell, *Chem. Soc. Rev.*, 1974, **3**, 513–544.
31 A. Bottoni, P. D. Casa and G. Poggi, *J. Mol. Struct. (Theochem)*, 2001, **542**, 123–127.
32 (*a*) T. D. Crawford and J. F. Stanton, *J. Chem. Phys.*, 2000, **112**, 7873–7879; (*b*) K. L. Bak, P. Jørgensen, J. Olsen, T. Helgaker and J. Gauss, *Chem. Phys. Lett.*, 2000, **317**, 116–122; (*c*) P. G. Szalay and J. Gauss, *J. Chem. Phys.*, 1997, **107**, 9028–9038; (*d*) W. Chen and H. B. Schlegel, *J. Chem. Phys.*, 1994, **101**, 5957–5968; (*e*) J. F. Stanton, *J. Chem. Phys.*, 1994, **101**, 371–374.
33 A. B. Sullivan, *J. Org. Chem.*, 1966, **31**, 2811–2817.
34 (*a*) I. Komaromi and J. M. J. Tronchet, *J. Phys. Chem.*, 1995, **99**, 10213–10220; (*b*) V. Barone, A. Grand, C. Minchino and R. Subra, *J. Phys. Chem.*, 1993, **97**, 6355–6361.
35 A. Ricca, J. Weber, M. Hanus and Y. Ellinger, *J. Chem. Phys.*, 1995, **103**, 274–280.
36 (*a*) R. Brière, H. Lemaire and A. Rassat, *Tetrahedron Lett.*, 1964, **27**, 1775; (*b*) H. Lemaire and A. Rassat, *J. Chem. Phys.*, 1964, **61**, 1580; (*c*) R. Brière, H. Lemaire and A. Rassat, *Bull. Soc. Chim. Fr.*, 1965, 3273.
37 (*a*) A. G. Kutzeladze, *J. Am. Chem. Soc.*, 2001, **123**, 9279–9282; (*b*) B. F. Minaev and H. Ågren, *J. Mol. Struct. (Theochem)*, 1998, **434**, 193–206.
38 (*a*) G. Rousseau, G. LePerche and P. M. Conia, *Tetrahedron Lett.*, 1977, 2517; (*b*) M. Orfanopolous, M. J. Grdina and L. M. Stephenson, *J. Am. Chem. Soc.*, 1979, **101**, 275; (*c*) K. H. Schulte-Elte and V. Rautenstrauch, *J. Am. Chem. Soc.*, 1980, **102**, 1738; (*d*) M. Prein and W. Adam, *Angew. Chem., Int. Ed. Engl.*, 1996, **35**, 477–494.
39 D. A. Singleton, C. Hang, M. J. Szymanski, M. P. Meyer, A. G. Leach, K. T. Kuwata, J. S. Chen, A. Greer, C. S. Foote and K. N. Houk, *J. Am. Chem. Soc.*, 2003, **125**, 1319–1328.